Elastography of Biological Tissue: Direct Inversion Methods That Allow for Local Shear Modulus Variations

C. Antonio Sánchez[1], Corina S. Drapaca[2], Sivabal Sivaloganathan[1,3], and Edward R. Vrscay[1]

[1] Department of Applied Mathematics, Faculty of Mathematics, University of Waterloo, Waterloo, ON, Canada
[2] Department of Engineering Science and Mechanics, Penn State Center for Neural Engineering, Pennsylvania State University, University Park, PA, USA
[3] Centre for Mathematical Medicine, Fields Institute, Toronto, ON, Canada
c.antonio.sanchez@gmail.com, csd12@psu.edu, ssivalog@uwaterloo.ca, ervrscay@uwaterloo.ca

Abstract. In recent years, imaging techniques have been adapted to indirectly measure stiffness of biological tissues, with the hope of using this information to aid in detecting and classifying pathological regions. Several methods have been developed to convert a sequence of strain images into a single elasticity image, but most are based on assumptions that limit the local variability of stiffness in the estimate. In this paper, two direct inversion methods are introduced. The novelty of these methods is that they concurrently solve a system of differential equations for the stiffness, allowing for strong local variations. Some ideas regarding uniqueness of solutions, an issue that is ignored in existing works, are also presented. Preliminary numerical results show that by keeping the differential terms in the tissue model, the new inversion methods can more accurately determine the tissue's stiffness distribution.

1 Introduction

It has been well known for millenia that the presence of abnormally stiff regions in a biological tissue is a strong indicator of damage or disease. Palpation has been the primary diagnostic procedure used since the days of Hippocrates [1], and is still one of the most common and efficient methods for detecting pathology in some soft tissues (such as tumours or cysts in the breast). This method, however, is limited to tissues near the surface of the body. In order to non-invasively examine tissues not accessible by touch, imaging techniques must be employed. Conventional imaging procedures are not able to discern pathological tissue from the surrounding healthy tissue if the two have similar molecular densities. This has led to the development of elastography techniques, which combine imaging with tissue mechanics in order to estimate stiffness values.

Magnetic Resonance Elastography (MRE) is a recently developed medical imaging technique used to non-invasively 'measure' mechanical properties of tissue [2]. The result is an image that quantitatively describes stiffness, and can be

A. Campilho and M. Kamel (Eds.): ICIAR 2010, Part II, LNCS 6112, pp. 195–206, 2010.

used by clinicians to diagnose or classify pathology. The MRE method consists of the following steps: (i) apply a known stress to the tissue, (ii) measure the physical response using MR phase-differencing [2], and (iii) invert a mathematical model that describes the mechanical behaviour of the tissue to find the desired stiffness parameters. Inversion can be performed using the measured data directly in the model [3,4,5], or indirectly with the use of an iterative technique [6,7]. In this paper, direct methods are considered.

The standard model is a system of differential equations that describes tissue motion in response to an applied stress. Inverting such a system can be difficult due to a lack of proper boundary conditions for stiffness, which cannot be measured due to the non-invasive nature of the experiment. To avoid this issue, simplifying assumptions are typically imposed when using direct methods, the most common of which is that the mechanical parameters can be locally approximated by constant functions [3,4,5]. In this case, the system of differential equations is converted into an algebraic system in terms of the unknown mechanical parameters, which can be easily solved using well-known matrix methods. The assumption, known as *local homogeneity*, limits the local variability of the parameters in the estimate. Furthermore, wherever the true parameters do vary significantly, the estimate is invalid. From a clinician's point-of-view, regions where the true stiffness changes rapidly are perhaps the most important, for they indicate the boundaries of any pathology.

In this paper, two novel direct methods are proposed to solve the system of differential equations, rather than the algebraic approximation. In the first method, the differential system is set as an equality constraint, and optimization methods are used to steer any free parameters. The second technique uses Green's functions to solve the system of differential equations. By solving the system of differential equations, a more accurate description of the stiffness parameters can be obtained, allowing for strong local variations. The result is an elastogram of more practical utility.

The structure of the paper is as follows. In Section 2, the tissue model is presented, and a few simplifying assumptions are used to reduce the number of free parameters. In Section 3, the issue of uniqueness of solutions is discussed. The novel methods are described in Sections 4 and 5, and preliminary results are presented for both simulated and measured data. The paper ends with some concluding remarks.

2 The Tissue Model

In this work, the tissue is modelled as a linearly viscoelastic isotropic continuum undergoing harmonic motion. To induce harmonic motion, a sinusoidal shear stress is applied to the boundary of the tissue near the region of interest, and the system is allowed to reach a quasi-steady state. The harmonic assumption is required for the MR phase-difference data acquisition technique [2]. An example of a measured displacement field is shown in Fig. 1. A linear constitutive law is adopted since the displacements have very low amplitudes (on the order of micrometres). With these assumptions, the equations of motion, written in the frequency domain, are the following:

$$-\omega^2 \rho \boldsymbol{U} = \nabla \cdot \left(\mathcal{M} \left[\nabla \boldsymbol{U} + \nabla^{\mathrm{T}} \boldsymbol{U} \right] \right) + \nabla \left(\Lambda \nabla \cdot \boldsymbol{U} \right) \quad , \tag{1}$$

where ω is the frequency of excitation, ρ is the density of the tissue, $\boldsymbol{U}$ is the three-dimensional harmonic displacement field, and Λ and $\mathcal{M}$ are complex, frequency-dependent versions of Lamé's first and second parameters. The vector differential operators act in such a way that the dimensions are consistent, and $\nabla^{\mathrm{T}} \boldsymbol{U} = [\nabla \boldsymbol{U}]^{\mathrm{T}}$. Equation (1) is a system of three differential equations with three unknown functions: ρ, Λ and $\mathcal{M}$. Without specifying some form of boundary or regularizing conditions, these three functions cannot be uniquely determined. The second Lamé parameter, $\mathcal{M}$ (also referred to as the complex shear modulus), is the parameter of interest since it has been experimentally shown to vary strongly with pathology [2,4,5].

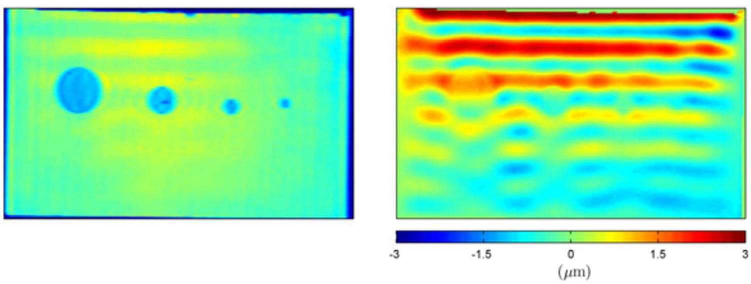

Fig. 1. Harmonic excitation of a gel phantom containing four stiff cylindrical inclusions: MR magnitude image (left) and the displacement pattern estimated from a sequence of MR phase-difference images (right). The experiment was performed in Dr. Richard Ehman's MRE lab at the Mayo Clinic [8].

In order to limit the number of free parameters in the system, two of the unknown functions are eliminated. Soft tissues are mainly composed of water, so the density is usually assumed to be constant with a value of $1\,\mathrm{g/cm^3}$. The large presence of water also causes the tissue to be nearly incompressible; thus, the longitudinal component, $\nabla \left(\Lambda \nabla \cdot \boldsymbol{U} \right)$, is expected to be negligible. With these two further assumptions, the system is reduced to

$$-\omega^2 \boldsymbol{U} = \mathcal{M} \, \nabla \cdot \left(\nabla \boldsymbol{U} + \nabla^{\mathrm{T}} \boldsymbol{U} \right) + \nabla \mathcal{M} \cdot \left(\nabla \boldsymbol{U} + \nabla^{\mathrm{T}} \boldsymbol{U} \right) \quad , \tag{2}$$

where the only unknown function is the desired shear modulus, $\mathcal{M}$, and the equations have been expanded using a vector calculus identity. If the local homogeneity assumption is imposed, then $\nabla \mathcal{M}$ is forced to be zero everywhere. The result is an algebraic expression for the shear modulus that can be solved using least-squares. This approach is known as Algebraic Inversion of the Differential Equation (AIDE) [5,9]. In this paper, however, the gradient of the shear modulus is not ignored. Two novel techniques are proposed to invert the system of differential equations in (2). If the combination of the three equations in the system does not provide enough information to determine a unique solution, then regularizing assumptions are invoked to isolate a particular one.

3 Uniqueness

If the mathematical model accurately describes the tissue of interest, then there is a theoretical 'true' distribution of the complex shear modulus. The goal of elastography is to determine this modulus using the measured displacement data. If there is not enough information to determine a unique solution, then further assumptions must be made. However, the determined solution will only be accurate if the assumptions are valid. As soon as assumptions like local homogeneity are imposed, there is no guarantee that a good approximation to the true solution will be found.

Uniqueness has not been thoroughly explored in existing MRE literature. It has been strongly suggested that including the $\nabla\mathcal{M}$ term in the inversion procedure requires the boundary conditions to be known [5,9]. However, mathematical analysis shows that this is not necessarily true; there exist local conditions for which (2) has a unique solution, without the need for boundary conditions. The differential system, ignoring density and the longitudinal component, can be expressed in matrix form as follows:

$$\left[\nabla\cdot\left[\nabla\boldsymbol{U}+\nabla^{\mathrm{T}}\boldsymbol{U}\right]\ \left[\nabla\boldsymbol{U}+\nabla^{\mathrm{T}}\boldsymbol{U}\right]\right]\begin{bmatrix} I \\ \nabla^{\mathrm{T}}\end{bmatrix}\mathcal{M}=-\omega^2\boldsymbol{U}\ , \tag{3}$$

where I is the identity operator. Note that this is a system of three equations involving four unknown terms: $\mathcal{M}$, $\frac{\partial\mathcal{M}}{\partial x}$, $\frac{\partial\mathcal{M}}{\partial y}$, and $\frac{\partial\mathcal{M}}{\partial z}$. Also, note that the coefficients of the differential operator depend on the displacement field, $\boldsymbol{U}$. A consequence of this is that if a second, linearly independent displacement field is obtained (perhaps by repeating the experiment while changing the location of the shear stress), enough equations are generated to locally estimate all unknown terms. Without repeating the experiment, there are additional conditions that still guarantee uniqueness, at least locally. For example, for all points satisfying

$$\operatorname{rank}\left\{\left[\nabla\boldsymbol{U}+\nabla^{\mathrm{T}}\boldsymbol{U}\right]\right\}<\operatorname{rank}\left\{\left[\nabla\cdot\left[\nabla\boldsymbol{U}+\nabla^{\mathrm{T}}\boldsymbol{U}\right]\ \left[\nabla\boldsymbol{U}+\nabla^{\mathrm{T}}\boldsymbol{U}\right]\right]\right\}\ , \tag{4}$$

$\mathcal{M}$ is uniquely determined. This condition allows for $\nabla\mathcal{M}$ to be removed using local Gaussian elimination techniques, leaving an expression involving only $\mathcal{M}$. If $\left[\nabla\boldsymbol{U}+\nabla^{\mathrm{T}}\boldsymbol{U}\right]$ has full rank, then another condition that guarantees local uniqueness is

$$\nabla\times\left[\left[\nabla\boldsymbol{U}+\nabla^{\mathrm{T}}\boldsymbol{U}\right]^{-1}\nabla\cdot\left(\nabla\boldsymbol{U}+\nabla^{\mathrm{T}}\boldsymbol{U}\right)\right]\neq 0\ . \tag{5}$$

With Condition (5), it can be shown that the only consistent solution to the homogeneous problem is the zero solution, which guarantees uniqueness of the inhomogeneous problem [10]. Thus, for any local regions where either of (4) or (5) hold, the system in Equation (2) can be locally inverted without the need for boundary conditions. In these instances, the system is known as being *completely integrable* in the Frobenius sense [11].

There are cases, however, where the solution is not unique. For example,

$$\boldsymbol{U} = \begin{bmatrix} e^{ikx} \\ e^{iky} \\ e^{ikz} \end{bmatrix} \quad \Longrightarrow \quad \mathcal{M} = \frac{w^2}{2k^2} + \alpha\, e^{-ik(x+y+z)}, \quad \text{for any } \alpha \in \mathbb{C} \ .$$

Thus, there is a family of solutions with one free parameter, α. A regularizing condition must be enforced in order to isolate a particular solution. This will only match the true solution if the assumptions are valid. Physically, the complex shear modulus should satisfy $\mathrm{Re}\{\mathcal{M}\} > 0$ and $\mathrm{Im}\{\mathcal{M}\} \geq 0$, which forces α to be zero. Thus, based on physically justifiable assumptions, the true solution might still be uniquely determined.

The family of solutions to the system in (2) has very few free parameters to begin with, if any. Assumptions like local homogeneity, while convenient, are not always required. By enforcing them, one is limiting the accuracy of the inversion method. To accurately capture strong variations in the shear modulus, it might be best to attempt to solve the differential system instead of the algebraic approximation, then impose regularizing conditions as a last resort to set any free parameters.

4 Direct Inversion Using Optimization Techniques

In order to solve (2) for the complex shear modulus, the problem is re-posed in a constrained optimization framework:

$$\begin{aligned} &\textit{Minimize} \quad f(\mathcal{M}) = \|\nabla\mathcal{M}\|^2 \ , \\ &\textit{subject to the equality constraint given by } (2) \ . \end{aligned}$$

Inequality constraints, such as $\mathrm{Re}\{\mathcal{M}\} > 0$ and $\mathrm{Im}\{\mathcal{M}\} > 0$, can also be imposed. The equality constraint guarantees that the the complex shear modulus satisfies the equations of motion. The quadratic minimization functional, f, then sets the free parameters in order to select a particular solution out of the space of admissible ones. Even though the condition that $\|\nabla\mathcal{M}\|^2$ be minimized is similar to the local homogeneity assumption, $\nabla\mathcal{M} = 0$, this optimization method is fundamentally different from AIDE. Here, one is searching for the particular solution among the set of admissible solutions that is the most locally homogeneous. In the AIDE technique, local homogeneity is enforced before the inversion is performed, and the resulting estimate will not be found in the set of admissible solutions if the true shear modulus varies at all.

To minimize computational complexity, inversion is performed on local block domains, similar to Van Houten's subzone approach [6]. On these domains, derivative operators acting on $\mathcal{M}$ are represented by discrete approximations, such as finite-difference matrices, with the boundary conditions left as free parameters. This can be accomplished by setting to zero all rows in the finite-difference matrices that correspond to boundary points. A simple null-space method is used to steer any free parameters if the discretized version of (2) is not invertible. Otherwise, the system is solved using least-squares.

4.1 Results

Simulated Data
Two simulated displacement fields were generated by solving the full three-dimensional forward problem of (2) for $\boldsymbol{U}$, given a known distribution of the shear modulus, $\mathcal{M}$. In the first simulated test-case, a spherical inclusion was introduced in the centre of the domain, with a stiffness value of $\mathrm{Re}\{\mathcal{M}\} = 7\,\mathrm{kPa}$. The background stiffness was taken to be 3 kPa, and a linear transition was introduced around the boundary of the inclusion to ensure continuity. In the second simulated test-case, a Gaussian bump was added to the centre of the domain with background stiffness of 3 kPa, to have a peak of 7 kPa. Sinusoidal variations were then introduced everywhere to test the impact of local variations. The volume of the simulated tissue is $10 \times 10 \times 4.8\,\mathrm{cm}$, with grid dimensions $128 \times 128 \times 24$. A sinusoidal shear force was applied to one side of the tissue, with an amplitude of $1\,\mu\mathrm{m}$ at a frequency of 100 Hz. Absorbing boundary conditions were implemented using a perfectly matched layer adapted to the elastic wave equation [10,12]. The first harmonic was extracted using a Fast Fourier Transform, and this was fed into the new inversion algorithm.

The inversion was performed on $20 \times 20 \times 20$ blocks, with a 50% overlap. Solutions in overlapping regions were averaged together to ensure smooth transitions. Savitzky-Golay filters were used to estimate derivatives of the data [13]. Fourth-order centred finite difference matrices were used to represent the derivative operators acting on $\mathcal{M}$, with the boundary conditions left free. For these two simulated test-cases, it was found that the discretized version of (2) was a fully determined system, implying the solution is unique. Results are shown in Fig. 2. The shear modulus estimates from the new method are significantly more accurate than those obtained using the traditional AIDE technique. In AIDE, the shear modulus distribution is deformed for both test-cases, and a ringing behaviour is exhibited at the boundary of the spherical inclusion of the first test-case. By allowing local variations in $\mathcal{M}$, the sharp transition about the spherical inclusion can be accurately determined, and the true shapes of the stiffness maps are preserved.

Experimental Data
Measurements of a three-dimensional displacement field were obtained from an experiment on a gel phantom containing four cylindrical stiff inclusions. The background gel was 1.5% Agar, having a stiffness of approximately 2.9 kPa, and the four cylindrical inclusions were composed of 10% B-gel (bovine), with a

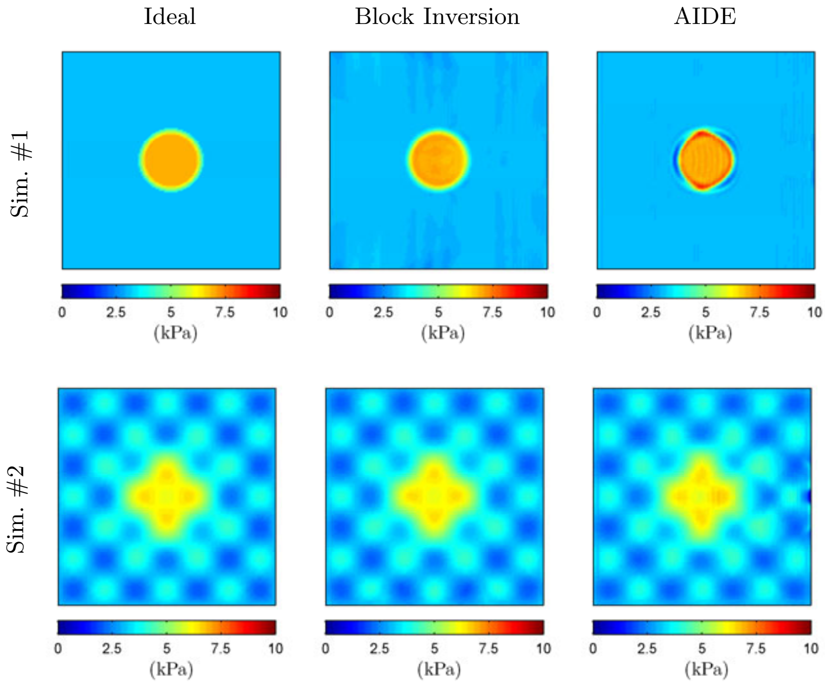

Fig. 2. Centre slice, parallel to the xy-plane, of the real component of the complex shear modulus for two simulated test-cases. Waves are travelling from left to right in the simulated displacement fields.

stiffness of approximately 6.4 kPa. The diameters of the four cylinders were approximately 5, 10, 16 and 25 mm. The field of view was 20×20 cm with a slice thickness of 3 mm. The grid dimensions were $256 \times 256 \times 16$. A sinusoidal force was applied to one side of the domain with an amplitude of 2 μm at a frequency of 100 Hz. The displacement field was measured using a MR phase-difference technique. This experiment was performed by Dr. Richard Ehman's MRE lab at the Mayo Clinic [8]. The data was preprocessed with a third-order Savitzky-Golay smoothing filter to remove noise, and was trimmed to contain $188 \times 98 \times 14$ points. The first harmonic was extracted using a Fast Fourier Transform.

Inversion was performed on $20 \times 20 \times 14$ blocks, with 50% overlap. Again, Savitzky-Golay filters were used to estimate derivatives of the data, and the derivative operators acting on $\mathcal{M}$ were represented by fourth-order centred finite difference matrices with boundary conditions left as free parameters. Similar to the simulated test-cases, the solution was determined to be unique. The estimates using the new method and AIDE are shown in Fig. 3. Again, one can see that the estimate from the new method is more accurate, particularly in and around the stiff inclusions, than that from AIDE. The AIDE result continues to show a ringing behaviour at sharp transitions of the shear modulus. This is caused by the local homogeneity assumption; in these regions of sharp variation, the assumption breaks down, rendering the shear modulus estimate invalid. The AIDE result, however, is smoother, particularly in the background region. This is because the local homogeneity assumption also regularizes, smoothing the solution. No such regularization is performed in the new block inversion method, making it more sensitive to background noise.

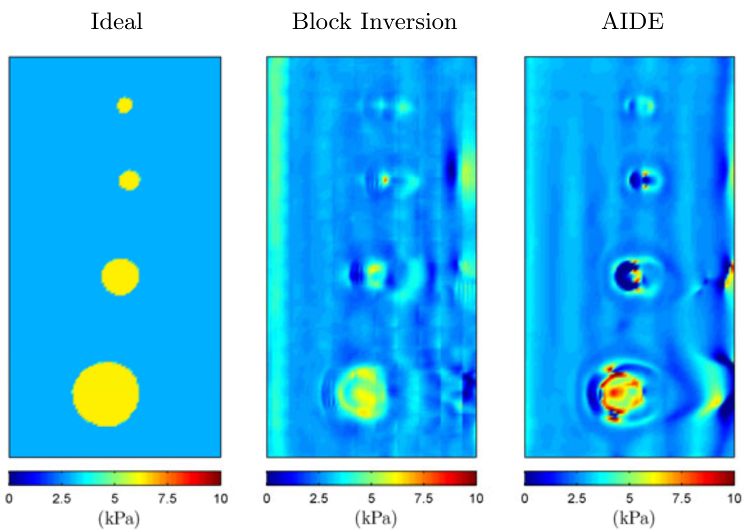

Fig. 3. Centre slice, parallel to the xy-plane, of the real component of the complex shear modulus for a the experimental data. Waves are travelling from left to right in the measured displacement field.

5 Direct Inversion Using Green's Functions

Both the AIDE and block inversion methods require knowledge of second-order derivatives of the displacement data. In practice, the measured data will contain noise, which is amplified by differentiation. This can make inversion methods unstable. The block inversion method presented in the previous section is particularly sensitive to variations in the data, so heavily relies on preprocessing techniques. To reduce this sensitivity, the need to estimate high-order derivatives of the data must be eliminated. This can be accomplished with the use of a Green's function.

Green's functions are used extensively in the study of Partial Differential Equations (PDEs), and are extremely useful in solving inhomogeneous problems subject to known boundary conditions. If a Green's function for a particular differential operator exists, then the PDE can be inverted using a convolution. To demonstrate this concept, consider the following simplified equations:

$$-\omega^2 \boldsymbol{U} = \nabla^2 \left(\mathcal{M} \boldsymbol{U} \right) \quad . \tag{6}$$

In order to arrive at this Helmholtz system, it must be assumed that the tissue is locally homogeneous and completely incompressible. However, like the previous method, the complex shear modulus is expressed in a system of differential equations with unknown boundary conditions. The free-space Green's function for the 3D Laplacian operator is given by

$$\mathcal{G}(\boldsymbol{x}) = -\frac{1}{4\pi\|\boldsymbol{x}\|} \ .$$

A convolution with this Green's function will invert a Laplacian provided the function decays rapidly at the extremes. Unfortunately, the convolution is defined on all $\mathbb{R}^3$, but the data is only known in some finite region. Thus, either the Green's function must be modified to account for the finite boundary, or a data window must be introduced. To prevent the need to numerically determine a Green's function based on the data, the latter approach is used. Both sides of (6) are multiplied by a window function, W, that has compact support. A convolution with the Green's function, $\mathcal{G}$, is then performed, resulting in the following system:

$$-\omega^2\,\mathcal{G} * (W\boldsymbol{U}) = \mathcal{M}\,W\boldsymbol{U} - \underbrace{\mathcal{G} * \left(2\nabla W \cdot \nabla\left(\mathcal{M}\boldsymbol{U}\right) + \mathcal{M}\boldsymbol{U}\nabla^2 W\right)}_{\mathcal{B}} \ . \qquad (7)$$

If W is discontinuous, then derivatives must be considered in the sense of distributions. A typical example of a window is the boxcar function, which has a value of one in some interior region, and zero outside. With a 3D boxcar window, the boundary term, $\mathcal{B}$, depends on the values of $\mathcal{M}$ and its derivatives at the boundaries. Unfortunately, this means boundary conditions on $\mathcal{M}$ are required in order to evaluate the expression given in (7).

As an initial estimate, it is assumed that the complex shear modulus is constant over the boundaries of the data window. With this assumption, $\mathcal{M}$ can be pulled outside of the boundary term, allowing the initial estimate to be expressed as follows:

$$\mathcal{M}^{(1)} = -\frac{\omega^2\mathcal{G} * (W\boldsymbol{U})}{W\boldsymbol{U} - \mathcal{G} * (2\nabla W \cdot \nabla\boldsymbol{U} + \boldsymbol{U}\nabla^2 W)} \ .$$

This only involves first derivatives of the data, resulting in a more stable system. In this way, three estimates of the shear modulus are obtained, one from each of the three equations of motion. These should be combined using a weighted averaging scheme, like least-squares. The estimate can then be iteratively improved by using the boundary values found in the previous iteration:

$$\mathcal{M}^{(k)} = -\frac{\omega^2\mathcal{G} * (W\boldsymbol{U})}{W\boldsymbol{U} - \mathcal{G} * \left(2\nabla W \cdot \nabla\left(\mathcal{M}^{(k-1)}\boldsymbol{U}\right) + \mathcal{M}^{(k-1)}\boldsymbol{U}\nabla^2 W\right)} \ ,$$

where k is the iteration number. In this way, it is hoped that the complex shear modulus will converge to a solution that satisfies the system given in (7). If the system of differential equations has any degrees of freedom, then further regularizing assumptions must be included in the iterative procedure to steer any free parameters and guarantee convergence.

Preliminary Results

The Green's function method was applied to the two simulated displacement fields and the one measured displacement field. Derivatives of the data window and Green's function were analytically determined, then discretized. For these preliminary results, only the first estimate, $\mathcal{M}^{(1)}$, is reported. A small window with a $5 \times 5 \times 5$ support was used in order to reduce the impact of the constant boundary assumption. The window was shifted one point at a time in order to simplify the inversion procedure, allowing the estimate to be expressed as a single ratio of two convolutions:

$$\mathcal{M}^{(1)} = -\frac{\omega^2 (W\mathcal{G}) * \boldsymbol{U}}{\nabla^2 (WG) * \boldsymbol{U}} \ .$$

A slice of the results is shown in Fig. 4.

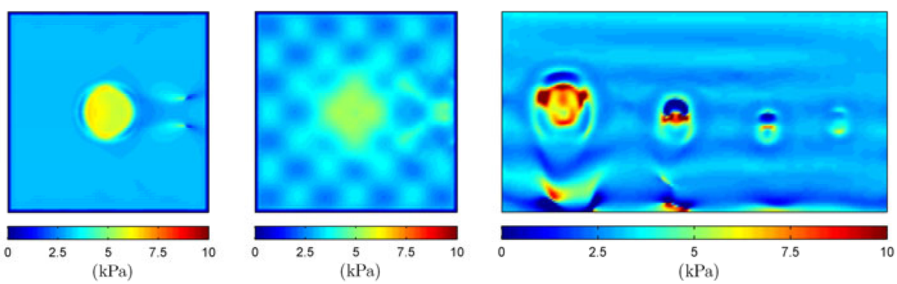

Fig. 4. Centre slice of the real component of the complex shear modulus for the three test-cases. Waves are travelling from left to right in the simulated displacement fields (left, centre), and top to bottom in the measured displacement field (right).

Since the simplified equation of motion is based on the local homogeneity and incompressibility assumptions, the accuracy of the shear modulus estimate is limited. Just as for the AIDE method, the sharp transitions about the inclusions in the first and third test cases cannot be accurately captured; the local homogeneity assumption introduces a ringing artifact in these regions. The incompressibility assumption also affects the estimated stiffness values, particularly within the regions of high stiffness for the two simulated cases. The advantage of this method, however, is that it is incredibly robust. Even with high levels of noise, reasonable estimates of the complex shear modulus can be obtained. The convolution acts as a smoothing operator, averaging noise that falls within the support of the data window.

In order to increase accuracy, the original system of equations, (2), should be used instead of the Helmholtz system. Unfortunately, the Green's function will depend on the displacement field, so will need to be determined numerically. The same iterative procedure can still be used, where an initial estimate of the shear modulus can provide boundary conditions for the next iteration. In this way, the system of differential equations can be solved using a Green's function.

6 Conclusions

Using theory for systems of PDEs, it can be shown that the equations relating the complex shear modulus to the displacement field, (2), can admit unique local solutions, without the need for regularizing assumptions or boundary conditions. When local homogeneity is imposed, the estimate of the shear modulus is rendered invalid in any regions where the true stiffness varies strongly. These regions mark the boundaries of any pathological tissue, so are important from a clinical perspective. By keeping the differential terms, a more accurate estimate of the true stiffness distribution can be obtained.

One approach to solving the system of partial differential equations is to leave the boundary conditions as free parameters, and use constrained optimization techniques to converge to a solution. In this way, the obtained solution is guaranteed to satisfy the original system, even in regions with local stiffness variations. This method has been found to produce more accurate estimates of the complex shear modulus than the traditional AIDE technique. However, the inversion is quite sensitive to noise. To reduce sensitivity, Green's functions can be employed. These functions are applied through a convolution, which has desireable numerical properties; noise is smoothed out over the region of integration, and derivatives of the data can be passed onto the Green's function, which helps stabilize the system. Boundary conditions are determined through an iterative procedure. The result is a very robust method to solve the system of PDEs. The 'best' method to use depends on the quality of the data. If it is relatively noise-free, then the optimization technique is the most straightforward and produces the most accurate estimate. If the data contains a lot of noise, then the more robust Green's function method provides a more reliable estimate of the complex shear modulus. By improving the accuracy of stiffness estimates, the resulting elastograms can be used more reliably in clinical applications, becoming part of a non-invasive tool to aid in the initial diagnosis of tissue pathology, and in tracking the progress of treatment strategies.

Acknowledgements

We gratefully acknowledge the generous support of this research by the Natural Sciences and Engineering Research Council of Canada (NSERC) in the forms of a Discovery Grant (ERV) and a Canada Graduate Scholarship (CAS). We would also like to thank Dr. Richard Ehman and his lab at the Mayo Clinic for the experimental data.

References

1. Bynum, W., Porter, R.: Medicine and the Five Senses. Cambridge University Press, Cambridge (2005)
2. Muthupillai, R., Lomas, D.J., Rossman, P.J., Greenleaf, J.F., Manduca, A., Ehman, R.L.: Magnetic resonance elastography by direct visualization of propagating acoustic strain waves. Science 269, 1854–1857 (1995)
3. Sinkus, R., Lorenzen, J., Schrader, D., Lorenzen, M., Dargatz, M., Holz, D.: High-resolution tensor MR elastography for breast tumour detection. Phys. Med. Biol. 45, 1649–1664 (2000)
4. Manduca, A., Oliphant, T.E., Dresner, M.A., Mahowald, J.L., Kruse, S.A., Amromin, E., Felmlee, J.P., Greenleaf, J.F., Ehman, R.L.: Magnetic resonance elastography: non-invasive mapping of tissue elasticity. Med. Image Anal. 5, 237–254 (2001)
5. Oliphant, T.E., Manduca, A., Ehman, R.L., Greenleaf, J.F.: Complex-valued stiffness reconstruction for magnetic resonance elastography by algebraic inversion of the differential equation. Magn. Reson. Med. 45, 299–310 (2001)
6. Van Houten, E.E., Miga, M.I., Weaver, J.B., Kennedy, F.E., Paulsen, K.D.: Three-dimensional subzone-based reconstruction algorithm for MR elastography. Magn. Reson. Med. 45, 827–837 (2001)
7. Van Houten, E.E., Doyley, M.M., Kennedy, F.E., Paulsen, K.D., Weaver, J.B.: A three-parameter mechanical property reconstruction method for MR-based elastic property imaging. IEEE Trans. Med. Imaging 24, 311–324 (2005)
8. Ehman, R.L.: Mayo Clinic Research: Magnetic Resonance Elastography (January 2007), `http://mayoresearch.mayo.edu/ehman_lab/mre.cfm`
9. Oliphant, T.E.: Direct Methods for Dynamic Elastography Reconstruction: Optimal Inversion of the Interior Helmholtz Problem. PhD in Biomedical imaging, Mayo Graduate School, Rochester, MN (2001)
10. Sánchez, C.A.: Dynamic Magnetic Resonance Elastography: Improved Direct Methods of Shear Modulus Estimation. MMath in Applied Mathematics, University of Waterloo, Waterloo, ON (2009)
11. Abraham, R., Marsden, J.E.: Foundations of Mechanics, 2nd edn. Addison–Wesley, California (1987)
12. Berenger, J.P.: Perfectly Matched Layer (PML) for Computational Electromagnetics. Morgan & Claypool Publishers, San Francisco (2007)
13. Savitzky, A., Golay, M.: Smoothing and differentiation of data by simplified least squares procedures. Analytical Chemistry 36, 1627–1639 (1964)